An Attitude Estimation Algorithm for Mobile Robots under Unknown Magnetic Disturbances

Digital Object Identifier 10.1109/TMECH.2016.2559941

IEEE/ASME TRANSACTIONS ON MECHATRONICS, VOL. TBD, NO. TBD, DATE TBD

An Attitude Estimation Algorithm for Mobile Robots Under Unknown Magnetic Disturbances

Riccardo Costanzi, Francesco Fanelli, Niccolò Monni, Alessandro Ridolfi, *Member, IEEE,* and Benedetto Allotta, *Member, IEEE*

***Abstract*—Attitude estimation is a crucial aspect for navigation and motion control of autonomous vehicles. This concept is particularly true in the case of unavailability of localization sensors, when navigation and control rely on dead reckoning strategies; in this case, indeed, the orientation estimate is also used along with speed measurements to update the position estimate. Among the different approaches proposed in the literature, the *de facto* state of the art in this field is represented by non-linear complementary filters: they fuse the measurements of angular rate obtained through gyroscopes and a measurement of gravity and Earth's magnetic field vectors respectively obtained through accelerometers and magnetometers. The described work is focused on an attitude estimation strategy for Autonomous Underwater Vehicles (AUV). The proposed novelty includes the identification of some critical issues that arise when AUV attitude estimation algorithms are applied in practice: they are mainly due to the use of low accuracy low cost Micro-Electro-Mechanical Systems (MEMS) sensors and on different sources of magnetic disturbances. Some strategies to overcome the identified issues are proposed, including the integration of a single axis Fiber Optic Gyroscope (FOG), that ensures a considerable performance improvement with a moderate cost increase. The proposed strategies for detection of issues and sensor fusion have been experimentally tested and validated in a real application scenario estimating the attitude of an AUV performing a lawn mower path. The expected performance improvement is confirmed; the obtained results are described and analyzed in the paper.**

***Index Terms*—AUV, complementary filter, marine robotics, underwater robots, orientation estimation.**

I. Introduction

The large diffusion of Micro-Electro-Mechanical Systems (MEMS) witnessed in recent years resulted in the spread of low cost and lightweight Inertial Measurement Units (IMUs); such components, together with suitable estimation algorithms employed to fuse the data acquired by the sensors, **supported the development of** a large number of Inertial Navigation Systems (INS), which are nowadays used in several different scientific fields.

One of the most common application of IMUs, usually composed of a three axes gyroscope and a three axes accelerometer and integrated with a three axes magnetometer, is the attitude estimation of mobile robots where they are mounted on. The robot attitude estimation is a crucial aspect for motion control, in particular when the navigation system is based on dead reckoning because of the lack of **global** localization systems. This is, e.g., the case of Autonomous Underwater Vehicles (AUV), that, because of the absorption of the radio waves by the water, cannot exploit the Global Positioning System (GPS).

Many sources regarding different filtering strategies of IMU signals for attitude estimation can be found in literature. **The classic approach consists in the use of a Kalman Filter (KF) [1] or of its nonlinear versions, such as the Extended Kalman Filter (EKF) or the Unscented Kalman Filter (UKF) [2], [3]. For instance, in [4] accelerometer and magnetometer measurements are fused in a KF structure to derive an asymptotically stable attitude estimation filter; in [5], [6] the authors propose a quaternion-based EKF, while in [7] a Sigma Point Kalman Filter (SPKF, the class of KF extensions whom the UKF belongs to) fusing GPS and INS data is used to overcome the problems due to linearization of the system dynamics and to the lack of knowledge of the initial estimate. An alternative to KFs is the employment of complementary filters, which can be used to fuse measurements possessing complementary spectral characteristics; for example, in [8] the authors exploit a low-frequency estimate obtained from accelerometer data and a high-frequency estimate computed from gyro readings.** One of the most important contributions to the subject has been given in [9], where the authors propose a filtering solution named Nonlinear Explicit Complementary Filter (NECF in the following), due to the structural similarity with linear complementary filters. NECF has become a standard reference in the field also thanks to a formal demonstration, through Lyapunov theory, provided in [9] about the convergence of the estimation to the real orientation. The approach is based on the possibility of measuring with respect to a frame moving with the vehicle at least two directions known in an Earth frame. The common strategy is to exploit the accelerometers for gravity acceleration direc-

Benedetto Allotta, Riccardo Costanzi, Francesco Fanelli, Niccolò Monni and Alessandro Ridolfi are with the Department of Industrial Engineering (DIEF), Mechatronics and Dynamic Modelling Laboratory (MDM Lab), University of Florence, Via di Santa Marta 3, 50139 Florence, Italy
Tel.: 0039 055 2758762
E-mails: [benedetto.allotta, riccardo.costanzi, francesco.fanelli, niccolo.monni, a.ridolfi] @unifi.it
Benedetto Allotta is a member of the Interuniversity Center of Integrated Systems for the Marine Environment (ISME)
Manuscript received TBD; revised TBD.

tion measurement (dynamics of an AUV is generally slow enough to consider negligible the proper acceleration with respect to the gravity one) and the magnetometers for Earth's magnetic field measurement.

In the application of this strategy on AUVs some issues may arise especially because of poor accuracy of the common low cost Micro-Electro-Mechanical Systems (MEMS) sensors and on different sources of magnetic disturbances. In this paper, the NECF is used as a basis and some integrations in the algorithm are proposed with the aim of better adapting the filter to attitude estimation of an underwater robot. The several possible sources of magnetic disturbance are analyzed; the identifiable ones are compensated in a calibration phase based on a strategy presented by the authors in a previously published work [10]. As concerns the magnetic disturbance due to local unidentifiable sources (e.g. survey of submerged modern wreck mainly composed of metal), an approach for detection and rejection of affected measurements, based on the signal of a single axis Fiber Optic Gyroscope (FOG), is proposed in this work.

The integration of a single axis FOG with this role in the overall attitude estimation algorithm ensures a considerable improvement of the performance, maintaining the costs affordable.

The proposed algorithm has been tested in a real application of autonomous navigation along a lawn mower path using FeelHippo AUV by the Mechatronics and Dynamic Modelling Laboratory (MDM Lab) of the Department of Industrial Engineering of the University of Florence (DIEF-UNIFI). According to the obtained experimental results, presented and commented in the paper, the expected performance improvement is confirmed; **the proposed algorithm succeeded in detecting and rejecting external unpredictable magnetic disturbances, at the same time computing a reliable attitude estimate.**

This paper is organized as follows: Section II introduces the system model describing the frames used in the following and the model of the dynamic behaviour of the IMU sensors and the FOG; Section III is dedicated to the description of the several possible magnetic disturbance sources and on the main concepts of the used calibration strategy proposed by the authors in a previous work [10]. Section IV presents the NECF: firstly the classic structure of the filter is illustrated; then, the applied design changes are introduced and justified. Finally, Section V presents the experimental results obtained and the derivable deductions.

II. System model

Throughout the paper, two suitable reference frames are used: the fixed frame N and the body frame B (Figure 1). The former is a North-East-Down frame [11], [12], while the latter is the frame attached to the IMU mounted on the vehicle; its x-axis is aligned with the direction of forward motion of the AUV, and the z-axis points down. The IMU considered in this paper is composed

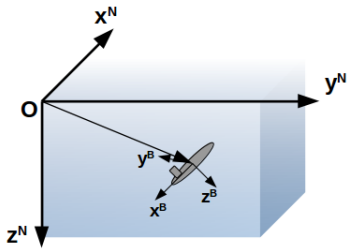

Fig. 1. NED reference frame

of a 3-axis gyroscope, a 3-axis magnetometer and a 3-axis accelerometer; the FOG is mounted with its sensitive axis aligned with the IMU z-axis. The orientation of the body frame with respect to the NED frame is expressed through the matrix $R = R_B^N$, from which a suitable triplet of Euler angles can be extracted. In this paper, roll pitch and yaw (RPY) angles, indicated respectively with ϕ, θ, and ψ, are used. The following error models are used to describe the functioning of the sensors:

- *Gyroscope*:

$$\boldsymbol{\omega}_m^B = \boldsymbol{\omega}^B + \mathbf{b}_g + \boldsymbol{\mu}_g \ , \tag{1}$$

  where the measured quantity $\boldsymbol{\omega}_m^B$ is the sum of the true angular velocity $\boldsymbol{\omega}^B$ expressed in the sensor frame, a time-varying bias $\boldsymbol{b}_g$ and additive measurement noise $\boldsymbol{\mu}_g$.
- *Magnetometer*:

$$\mathbf{m}_m^B = WR^T\mathbf{H}^N + \mathbf{H}_d + \boldsymbol{\mu}_m \ , \tag{2}$$

  being $\mathbf{H}^N$ the Earth's magnetic field expressed in the fixed frame, W and $\mathbf{H}_d$ represent the disturbances due to local magnetic interferences (whose effect will be analyzed in Section III) and $\boldsymbol{\mu}_m$ is measurement noise *(a similar magnetometer model can be found, for instance, in [13], [14], [15])*.
- *Accelerometer*:

$$\mathbf{a}_m^B = R^T\mathbf{a}^N + \mathbf{b}_a + \boldsymbol{\mu}_a \ , \tag{3}$$

  where $\boldsymbol{\mu}_a$ represents measurement noise and $\mathbf{b}_a$ is the accelerometer bias, responsible for a shift of the acceleration vector from its true direction (in this context, the accelerometer bias has been neglected). Vector $\mathbf{a}^N$, expressed in the frame N, is the sum of $\dot{\mathbf{v}}^N$, which is the time derivative of the linear velocity of the device $\mathbf{v}^N$, and of the gravitational acceleration $\mathbf{g}$. However, for the considered field of application, acceleration is usually very small; hence, the direction of $\mathbf{a}_m^B$ constitutes a good approximation of the fixed vertical axis expressed in the body frame.
- *FOG*:

$$\omega_m^{FOG} = \omega^{FOG} + b_e + b_F + \mu_F \ . \tag{4}$$

  ω^{FOG} is the true angular rate of the instrument, b_e is the component of Earth's rotation sensed by the gyro,

b_F is an additional bias term, and μ_F is measurement noise. Due to the high instrument resolution and accuracy, the sensor is capable of measuring Earth's rotation, whose effect is included in the term b_e (such bias can be nonetheless compensated, see Sec. IV-B4), while the remaining bias b_F is very low and can be often neglected during practical operation.

III. Magnetometer calibration

A 3-axis magnetometer measures the direction and the intensity of the total magnetic field around the device. It cannot, however, distinguish between the Earth's magnetic field and additive magnetic disturbances.

The Earth's magnetic field vector direction depends on the geographical location; however, over the operating area of an underwater vehicle, it can be considered constant with respect to the N frame; several online calculators are available to determine its components given the geographical latitude and longitude (e.g. [16]). In the absence of disturbances, the measurements (expressed in the body frame) obtained by arbitrarily rotating the sensor in every possible orientation would lie on the surface of a sphere with its center in the origin and whose radius is the magnitude of the field at the geographic location where such operation is performed. However, in the presence of magnets or ferromagnetic objects, the measurements locus is shifted and deformed.

Magnetic disturbances conceptually fall into two different categories: external (environmental) disturbances, and disturbances rotating together with the sensor. As regards the latter, they can be further characterized as Hard Iron or Soft Iron disturbances, whose effect is the following:

- *Hard Iron disturbances*:
  Permanent magnets and magnetized objects, such as electronic subsystems in the proximity of the sensor, give rise to the so-called "Hard Iron effect": these objects are the source of a permanent magnetic field, constant in all directions, whose effect is the addition of a constant bias $\mathbf{H}_d$ on the magnetometer output of the error model (2);
- *Soft Iron, scale factor and misalignment disturbances*:
  In this simplified (affine) error model, matrix W in Eq. (2) can be factored as follows:

$$W = W_{mis} W_{sf} W_{SI} \ . \tag{5}$$

  W_{mis} takes into account the misalignment between the axes of the sensor and the vehicle axes, including a non perfect orthogonality between the three axes of the magnetometer; W_{sf} models the different sensitivity of the device on its three axes, introducing a different scaling factor along the three directions; finally, W_{SI} represents the "Soft Iron effect": ferromagnetic materials close to the sensor, such as iron and nickel, produce a local magnetic field, whose magnitude is related to the angle of incidence of Earth's magnetic field on the material itself. Thus, this effect changes as the orientation of the sensor varies. All these contributions, combined into W, have the effect of deforming the measurements sphere into an ellipsoid, tilted in 3D space along an arbitrary axis.

If both kinds of disturbance are present, the measurements taken while rotating the sensor in space would lie on the surface of an ellipsoid (due to W) centered at a certain offset from the origin (due to Hard Iron effect).

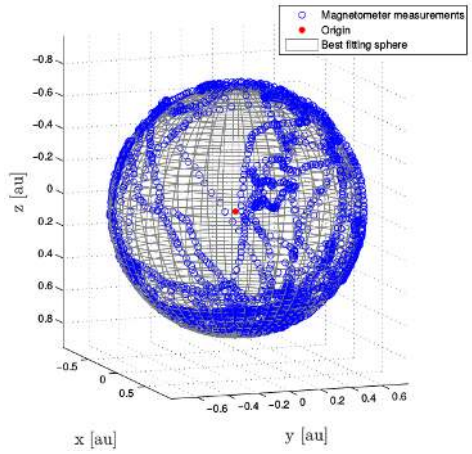

Fig. 2. Magnetometer readings with no magnetic disturbances, expressed in arbitrary units

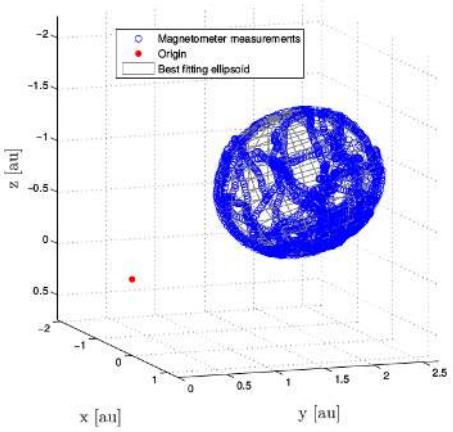

Fig. 3. Magnetometer readings with magnetic disturbances, expressed in arbitrary units

For instance, Figures 2-3 show the magnetometer measurements (expressed in the body frame) taken while rotating the device in 3D space. In the first case, the rotation was performed in a disturbance-free environment; the sensor readings lie with good approximation on the surface of a sphere with center in the origin. The radius of the sphere does not reflect the true magnitude of the magnetic field, since the measurements are given by the sensor in arbitrary units. On the other side, the measurements shown in Figure 3 were taken in the same geographical as in the previous test, but metal objects were preliminarily attached to the sensor case: it is easy to note the deformation of the previously obtained sphere into an ellipsoid and the shift its center is subjected to.

Magnetic disturbances rotating with the sensor can be completely compensated exploiting suitable calibration procedures; **for example, in [13], [14], the calibration process is cast as a maximum likelihood problem, and thus is solved using optimization tools, while in [15] a least square ellipsoid fitting algorithm is employed.** In this context, the calibration algorithm proposed by the authors in [10] has been used; such algorithm has been appropriately developed for use when rotation of the sensor about some axis is constrained. This is indeed the case of the majority of AUVs, whose physical structure dampens rotations about the body x- and y-axis. Such algorithm is appositely conceived to approximate at best the theoretical compass readings locus using only data acquired during a complete turn of the vehicle about its z-axis. For the detailed description of the calibration procedure, the reader is referred to [10]; in Section V, instead, the results obtained during two suitable validation tests of the calibration algorithm are reported.
On the other side, external disturbances cannot be neither compensated nor predicted; it is thus necessary to implement a suitable strategy in order to identify online and reject corrupted measurements, as described in Section IV-B3.

IV. NECF

A. NECF classic formulation

The attitude estimation filter adopted at the basis of this work is the explicit complementary filter proposed by Mahony et al., whose stability and convergence has been proved in 2008 [9]. This section offers a brief review of the standard formulation of the filter; then, the design changes applied to its original structure are explained.
At each iteration of the NECF, an estimate of the orientation of the IMU with respect to the fixed frame is computed; the filter integrates the angular rate changes along the tree axes measured by the gyroscope, and correct such quantities exploiting the accelerometer and magnetometer readings. If at least two fixed and nonparallel directions in the fixed frame can be measured with respect to the sensor frame, the algorithm converges to the exact attitude of the IMU. This condition is usually satisfied by commercial IMUs equipped with triaxial magnetometer and accelerometer. Particularly, assuming that the proper acceleration of the sensor is negligible (as it is usually the case with underwater robots) accelerometer readings give an estimate of the direction of the gravitational acceleration, and they are employed to correct the roll and the pitch integration; magnetometers measure the direction of Earth's magnetic field (i.e. they measure the direction of the North), and thus they can be used to compute an estimate of the yaw angle. Furthermore, the NECF also computes an estimate of the time-varying bias of the gyroscope.
The filter is a dynamical system governed by the following equations [9]:

$$\dot{\hat{R}} = \hat{R}\left(\left(\boldsymbol{\omega}_m^B - \hat{\mathbf{b}}_g\right)_\times + k_P\left(\boldsymbol{\omega}_{mes}\right)_\times\right), \quad \hat{R}(0) = \hat{R}_0 \tag{6}$$

$$\dot{\hat{\mathbf{b}}}_g = -k_I\boldsymbol{\omega}_{mes} \tag{7}$$

$$\boldsymbol{\omega}_{mes} = \sum_{i=1}^{n} k_i \mathbf{v}_i \times \hat{\mathbf{v}}_i, \quad k_i \geq 0, \quad i = 1, \cdots, n\ . \tag{8}$$

Concerning the notation, $\hat{\cdot}$ indicates an estimated value, $\hat{R}$ is an estimate of the rotation matrix which defines the attitude of the sensor (being $\hat{R}_0$ the initial estimate), k_P and k_I are tunable gains, and $(\mathbf{a})_\times$ is the operator that builds a skew-symmetric matrix from vector $\mathbf{a}$:

$$(\mathbf{a})_\times = \begin{bmatrix} 0 & -a_3 & a_2 \\ a_3 & 0 & -a_1 \\ -a_2 & a_1 & 0 \end{bmatrix}\ . \tag{9}$$

The term $\boldsymbol{\omega}_{mes}$ must be analysed in details: it is indeed the correction term built upon accelerometer and magnetometer measurements.
Let $\mathbf{v}_{0,i}$, with $i = 1, \cdots, n$, be a set of known fixed directions, and let

$$\mathbf{v}_i = R^T\mathbf{v}_{0,i} + \boldsymbol{\mu}_i \tag{10}$$

and

$$\hat{\mathbf{v}}_i = \hat{R}^T\mathbf{v}_{0,i} \tag{11}$$

denote, respectively, its measurement in the sensor frame (affected by noise $\boldsymbol{\mu}_i$) and its estimate (computed using the estimated rotation matrix $\hat{R}$); the term $\boldsymbol{\omega}_{mes}$ is the weighted sum of the misalignment between the measured directions and their estimates computed using the output of the filter. In particular, in the considered case the direction of the vertical axis (measured by the accelerometer) and the direction of the magnetic field (read by the magnetometer) are taken into account; the weights k_i are chosen according to the relative confidence in each measurement $\mathbf{v}_i$.
Let $\tilde{R} = \hat{R}^T R$ and $\tilde{\mathbf{b}}_g = \mathbf{b}_g - \hat{\mathbf{b}}_g$ denote, respectively, the orientation and gyro bias errors; then, for $n > 1$, Mahony et al. [9] have proven through the use of Lyapunov theory that $\left(\tilde{R}, \tilde{\mathbf{b}}_g\right)$ is locally exponentially stable to $(I, \mathbf{0})$.

B. Design changes

Using the measurements acquired by an IMU to estimate the attitude of an underwater vehicle through the NECF in its classic formulation (6)-(8), several issues arise. Hence, some design changes have been applied to the original structure of the filter in order to better adapt it to the underwater field of application. This section illustrates and justifies each applied modification; an experimental test campaign was conducted to verify the properties and effectiveness of the proposed method.

1) Filter on accelerometer measurements: Through suitable preliminary tests performed out of the water, it has been experimental observed that oscillating movements of the IMU on the horizontal plane cause undesired variations of the roll and pitch angles extracted from the output rotation matrix of the filter; this happens because the accelerometer interprets sudden horizontal movements of the sensor as deviations of the vertical direction, which in turn affect the computation of the rotation matrix. To produce accurate attitude estimates, this phenomenon must be identified and corrected in real-time. To smooth the obtained roll and pitch angles profiles and to reduce the amplitude of these variations, accelerations measurements have been filtered as follows:

$$\mathbf{a}_f = F(z)\mathbf{a}_m^B \ , \tag{12}$$

being $\mathbf{a}_f$ the filtered measurement, and $F(z)$ the transfer function of a suitable digital filter. Particular care has to be taken when choosing the filter order and cutoff frequency, since the result could be an undesirable delay of the estimated angles. Several filter with different cutoff frequencies have been tested; a second-order filter has then been adopted, constituting an effective trade-off between accuracy of the estimates and readiness of the NECF. **In particular, $F(z)$ is obtained by discretization of the filter with continuous transfer function**

$$F(s) = \frac{\omega^2}{(s+\omega)^2} \tag{13}$$

using the bilinear transform:

$$F(z) = F(s)|_{s=\frac{2z-1}{Tz-1}} \ , \tag{14}$$

being T the time between two subsequent filter iterations. For this particular application, the value $\omega = 2.5$ rad/s was chosen after suitable experimental tests. Note that, since only the direction of the acceleration vector is important, vector $\mathbf{a}_m^B$ is normalized before being filtered by $F(z)$; the same operation is executed on $\mathbf{a}_f$ before its use in $\boldsymbol{\omega}_{mes}$ (the notation has not been changed for the ease of reading).

2) Known directions choice: **Convergence of the classic NECF is demonstrated if the direction of at least two known nonparallel fixed vectors can be estimated in the sensor frame. Considering IMUs equipped with accelerometers and magnetometers, a common choice is to use the measurement of the gravitational acceleration (i.e. the vertical direction) and of the Earth's magnetic field (which points towards magnetic North, i.e. the x-axis of the fixed frame).** These quantities are used in the correction term $\boldsymbol{\omega}_{mes}$, where they are compared with the estimates of the chosen directions to generate an error term.

The proposed modification consists in choosing only the component of the measured magnetic field which is orthogonal to the acceleration direction instead of the complete magnetometer measurement (**please refer to Figure** 4; a similar approach can be found in [17], [18]). This choice

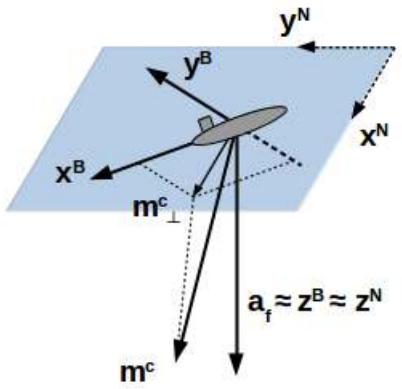

Fig. 4. Projection of the measured magnetic field on the plane orthogonal to acceleration

is justified by the following considerations: first of all, it is worth noting that the plane orthogonal to acceleration approximately coincides with the horizontal plane all the time; this is because the vehicle proper acceleration is usually negligible if compared to gravity, and because rotations along x-axis and y-axis are constrained. This means that the accelerometer readings give the direction of the fixed vertical direction $\mathbf{z}^N$ expressed in the body frame. In addition, accelerometer readings are less susceptible to external error sources than magnetometer readings, thus they are more reliable. Hence, even if no external magnetic disturbance is present, including the vertical component of the measured magnetic field does not produce further benefits with respect to using only the information carried by the acceleration estimate.

Thus, once the corrected compass readings $\mathbf{m}^c$ have been obtained through the calibration procedure, their projection onto the plane orthogonal to acceleration is computed:

$$\mathbf{m}_\perp^c = \mathbf{m}^c - \left(\left(\mathbf{a}_f\right)^T \mathbf{m}^c\right)\mathbf{a}_f \ . \tag{15}$$

Thanks to the previous observations, $\mathbf{m}_\perp^c$ (once expressed in the fixed frame) is a vector pointing towards North magnetic pole thus, after normalization, in $\boldsymbol{\omega}_{mes}$ it is compared with the estimate of the fixed north direction

$$\hat{\mathbf{x}}^N = \hat{R}^T \begin{bmatrix} 1 \\ 0 \\ 0 \end{bmatrix} \ . \tag{16}$$

3) Time varying gains: in Equation (8), the gains k_i of the correction term are constant and fixed before execution. However, during the normal functioning of the filter, unpredictable transitory errors may affect the measurements provided by accelerometers or magnetometers. These dangerous situations should be detected in real-time and the corresponding gains scaled according to the actual reliability of each measurement, in order to preserve the accuracy of the computed estimate.

In the considered case study, gains k_i are constant only during the initialization of the filter; in addition, it is worth remembering that the value of each gain is related to the reliability of the considered

measurement. In the underwater field of application, proper vehicle accelerations are small, while it is quite common to encounter sources of magnetic disturbance; hence, acceleration measurements will be, generally speaking, more reliable than compass readings. In view of these considerations, the accelerometer-related initial gain will be higher than its magnetometer-related counterpart. In order to discard unreliable measurements in real-time, these gains are eventually scaled over time (never exceeding the initial value). The procedure is different for the acceleration and the magnetic field readings.

a) Acceleration gain: In order to avoid that sudden accelerations along some directions generate a wrong contribute to the correction term of the filter (**Section** IV-B1), the acceleration gain k_1 is linearly decreased with the acceleration magnitude if high acceleration occurs. During the initialization, k_1 is fixed at the initial value determined through a preliminary tuning process, and the average value $\bar{a}$ of the magnitude of acceleration measurements is computed to be used as a reference term. Then, k_1 is set according to the relative distance between the norm of the acceleration measurement and $\bar{a}$:

$$D_a = \left| \frac{||\mathbf{a}_m^B|| - \bar{a}}{\bar{a}} \right| . \tag{17}$$

Referring to Figure 5: a_{th} represents the threshold value

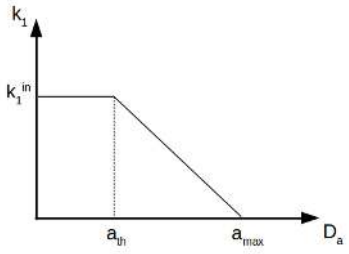

Fig. 5. Computation of gain k_1

which, if exceeded, causes the decrease of the gain until the maximum value a_{max} is reached, at which k_1 is set to zero. **Denoting with k_1^{in} the initial (constant) gain, k_1 is determined according to Algorithm** 1.

Data: k_1^{in}, a_{th}, a_{max}
Result: gain k_1
Compute D_a as in (17);
if $D_a < a_{th}$ **then**
  $k_1 = k_1^{in}$
else if $a_{th} < D_a < a_{max}$ **then**
  $k_1 = k_1^{in}\left(-\frac{1}{a_{max}-a_{th}} D_a + \left(1 + \frac{a_{th}}{a_{max}-a_{th}}\right)\right)$;
else
  $k_1 = 0$;
end

Algorithm 1: k_1 computation

b) Magnetic field gain: As stated in Section III, only disturbances which rotate with the sensor can be compensated, regardless of the calibration technique adopted. External metal objects are inevitably a source of magnetic disturbance that affects the yaw estimate. Their presence is not uncommon, especially in the field of underwater robotics: many AUVs are indeed used for inspection tasks of modern wrecks, mainly composed of metal parts and debris.
Since these disturbances cannot be corrected, the only possible countermeasure is to readily detect corrupted readings and to avoid the use of the magnetometer measurements in such situations, relying only on gyroscope integration for the yaw estimate.
The gain k_2 associated with the magnetometer readings is changed according to a different strategy with respect to the accelerometer gain k_1. Since it is likely that external disturbances modify the direction of the magnetic field without sensibly varying its magnitude, a magnitude-related law would be unreliable, leading to the use of wrong information for correction purposes. The idea is then to scale down k_2 if two particular angular constraints are violated **(please refer to Figure 6 for a better understanding)**. In the case that accurate gyroscope

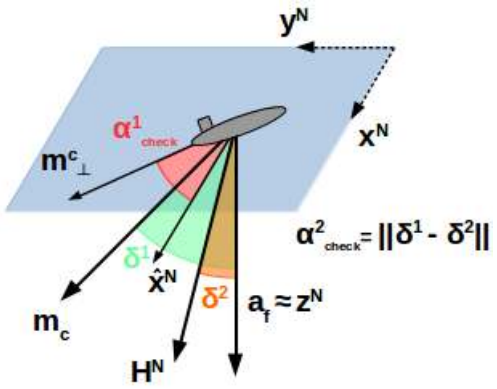

Fig. 6. Control angles associated with the magnetometer gain

data are available, on a brief period of time integration of the angular velocity leads to an error which is lower than the one generated by considering the corrupted magnetic measurements.
The first angle to be checked is the angle between the projection of the corrected measurement onto the plane orthogonal to the acceleration vector (which can be assumed to be the horizontal plane, see Sec. IV-B2) and the estimate of the x-axis:

$$\alpha_{check}^1 = cos^{-1}\left((\mathbf{m}_\perp^c)^T \hat{\mathbf{x}}^N\right) . \tag{18}$$

In ideal conditions, the magnitude of α_{check}^1 is zero (or, since sensors are affected by measurement noise, it has zero mean value). If a source of magnetic disturbance gets close to the sensor, the change in the magnetometer readings causes the estimated rotation $\hat{R}$ to vary. However, since the dynamics of the magnetometer are much faster than the filter, if the disturbance approaches the sensor sufficiently

rapidly a deviation of $\mathbf{m}_{\perp}^{c}$ is registered before a relevant change in $\hat{R}$ may occur, thus causing the increase of α_{check}^{1}. Nevertheless, the use of α_{check}^{1} only to verify the correctness of the magnetometer readings has a drawback: if the magnetic disturbance approaches the sensor very slowly, the velocity of the drift of the sensor reading may match the dynamics of the filter: in this case, a slow but continuous change in the yaw angle is registered, with α_{check}^{1} remaining close to zero even if a disturbance is present.

A second control angle α_{check}^{2} is thus introduced to overcome this problem. The choice of α_{check}^{2} is based on the following consideration: in a given geographical location the Earth's magnetic field can be considered constant: i.e. the angle between $\mathbf{H}^{N}$ and the vertical direction $\mathbf{z}^{N} = [0\ 0\ 1]^{T}$ is constant. The same angle must be measured between these vectors rotated in the body frame. Mathematically, this equality is expressed by the following relation:

$$\left(\mathbf{z}^{N}\right)^{T}\mathbf{H}^{N} = \left(\mathbf{a}_{f}\right)^{T}\mathbf{m}^{c}\ , \tag{19}$$

where the body frame vertical direction is given by the filtered accelerometer measurement.

Hence, α_{check}^{2} measures the angular distance between the angle $\left(\mathbf{a}_{f}\right)^{T}\mathbf{m}^{c}$ obtained at each iteration and the corresponding value $\left(\mathbf{z}^{N}\right)^{T}\mathbf{H}^{N}$:

$$\alpha_{check}^{2} = \left|\left| cos^{-1}\left(\left(\mathbf{a}_{f}\right)^{T}\mathbf{m}^{c}\right) - cos^{-1}\left(\left(\mathbf{z}^{N}\right)^{T}\mathbf{H}^{N}\right)\right|\right| . \tag{20}$$

The magnitude of α_{check}^{2} is independent from the speed at which a magnetic disturbance is applied. Note that, in Eq. (19) and Eq. (20), only the directions of the involved vectors are considered.

Two threshold values α_{th}^{1} and α_{th}^{2} are set; if either one is reached, k_2 is forced to zero in a finite number of iterations. If both angles fall below the threshold values, k_2 is increased back to the initial value. The decrease is much faster than the increase.

Let k^{u} and k^{d} be suitable increase and decrease counters, and let k_{max}^{u} and k_{max}^{d} denote the number of iterations allowed for the variation of the gain k_2. If k_2^{in} is the initial value for k_2, then Algorithm 2 illustrates how the magnetometer gain is computed. Even if no magnetic disturbances are present, it is possible for both angles to become greater than the threshold values; this can occur if large accelerations arise (which is not likely to happen in the field of underwater robotics) or during motion transients. However, this effect is only temporary and α_{check}^{1}, α_{check}^{2} fall again below the threshold in a short amount of time. This solution may appear quite conservative; nevertheless, if a precise gyroscope is available, it is indeed better to discard good magnetometer readings than running the risk of including corrupted magnetic measurements, thus compromising the accuracy of the yaw estimate.

In conclusion, in the considered case study $\boldsymbol{\omega}_{mes}$ has the following form:

$$\boldsymbol{\omega}_{mes} = k_1\mathbf{a}_f \times \hat{R}\mathbf{z}^{N} + k_2\mathbf{m}_{\perp}^{c} \times \hat{R}\mathbf{x}^{N}\ . \tag{21}$$

Data: k_2^{in}, k_{max}^{u}, k_{max}^{d}
Result: gain k_2
if $\alpha_{check}^{1} > \alpha_{th}^{1}$ *or* $\alpha_{check}^{2} > \alpha_{th}^{2}$ **then**
  $k_2 = k_2^{in}\left(1 - k^{d}/k_{max}^{d}\right)$;
  $k_2 \geq 0$;
  $k^{d}++$;
  $k^{u} = 0$;
else
  $k_2 = k_2 + \left(k_2^{in} - k_2\right)\left(k^{u}/k_{max}^{u}\right)$;
  $k_2 \leq k_2^{in}$;
  $k^{u}++$;
  $k^{d} = 0$;
end

Algorithm 2: k_2 computation

4) FOG integration: the majority of the commercial IMUs possess an internal algorithm that fuses the raw data coming from the sensors they are equipped with in order to estimate their own orientation. The use of a stand-alone attitude estimation filter yields the possibility of increasing the accuracy of the computed estimate by using data that come from sensors that are not originally built-in in the IMU. This is extremely useful in low cost applications, where cheaper MEMS sensors can be used together with more precise sensors. In the considered case, a single-axis Fiber Optic Gyroscope (FOG), an accurate and reliable sensor based on the Sagnac effect, has been mounted with its sensitive axis parallel to the IMU's gyroscope z-axis. Its measurement completely substitutes the axis angular rate change read by the IMU gyroscope within the estimation filter.

This choice is justified by the following consideration: the magnetometer related contribution in $\boldsymbol{\omega}_{mes}$ has the purpose of obtaining an accurate estimation of the yaw angle. In the case of magnetic disturbances the gain k_2 is set to zero, and the yaw estimate is obtained by raw integration of the angular velocity. Due to the bias of the IMU gyroscope, a relevant yaw drift is registered even if the sensor is not moving. However, since the FOG possesses a much lower bias than the IMU, the employment of its reading for the z-axis angular rate change allows to reach a high level of accuracy; through its use, the risk of unacceptable growth of the integration error when the magnetometer is not employed is avoided.

Nonetheless, the use of a FOG has a drawback: even if the component is not rotating, the device senses Earth's angular velocity, thus producing a nonzero output of up to 15° per hour. However, this effect can be compensated exploiting the knowledge of the latitude at which the sensor is operating and the information regarding the attitude of the vehicle.

Referring to Figure 7: it is assumed that the sensor is operating in the Earth's northern hemisphere; however, the compensation procedure is conceptually the same on the whole planet surface. Let $\boldsymbol{\omega}_E$ denote Earth's angular velocity; its magnitude, expressed in radians per second,

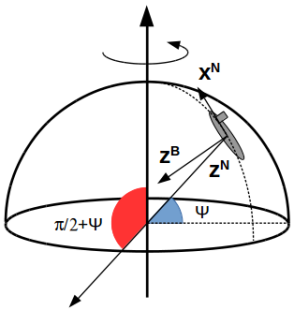

Fig. 7. FOG correction term computation

is then

$$\omega_E = ||\boldsymbol{\omega}_E|| \cong 7.2921 \cdot 10^{-5} \ . \tag{22}$$

The latitude Ψ is supposed to be known. The idea is to determine the component of Earth's angular rate acting on the body z-axis and subtract it from the sensor reading. At first, it is convenient to express Earth's angular velocity in the NED frame as follows:

$$\boldsymbol{\omega}_E^N = \begin{bmatrix} \omega_E cos\,(\Psi) \\ 0 \\ -\omega_E sin\,(\Psi) \ . \end{bmatrix} \tag{23}$$

Exploiting the current attitude estimate, one can compute the bias to be subtracted as the third component of the vector:

$$\boldsymbol{\omega}_E^B = \left(R_B^N\right)^T \boldsymbol{\omega}_E^N \ . \tag{24}$$

In conclusion, the corrected FOG measurement is given by:

$$\omega_c^{FOG} = \omega^{FOG} - \omega_E^B(3) \ . \tag{25}$$

After the correction has been applied, highly accurate measurements can be obtained: in the considered case study, mere integration over time of the compensated measurement while the device was held still showed an angle drift of about 2° per hour.

V. Test Results

The performance of the proposed filter has been evaluated on the FeelHippo AUV, developed and built by the MDM Lab of the University of Florence for the participation in the European robotic challenge SAUC-e 2013[1], thanks to the experience of the MDM Lab gained during the THESAURUS[2] and the ARROWS[3] projects [22]. Recently, FeelHippo has been substantially renovated for the participation in the robotic competition euRathlon 2015[4] (Figure 8). Table I resumes the main characteristics of the vehicle. The vehicle is equipped with a Xsens Technologies MTi-G-700 INS and a single-axis KVH DSP-1760 Fiber Optic Gyro mounted with its sensitive axis pointing down (Figure 9). Mounting both sensors on a rigid panel allowed to obtain a very limited misalignment

[1]SAUC-e competition: *www.sauc-europe.org*
[2]THESAURUS project: *www.thesaurus.isti.cnr.it*
[3]ARROWS project: *www.arrowsproject.eu*
[4]euRathlon 2015 competition: *www.eurathlon.eu*

Fig. 8. FeelHippo AUV at euRathlon 2015.

FeelHippo AUV characteristics	
Size [mm]	600×640×450 approx.
Mass [kg]	50
Max speed [kn]	2
Max depth [m]	30
Autonomy [h]	4
Navigation sensors	GPS, IMU, FOG, DVL, depth sensor, acoustic modem
Payload	cameras, 2D forward-looking sonar

TABLE I
FeelHippo AUV physical data, payload and performance.

error between the FOG sensitive axis and the IMU z-axis, which did not cause issues during the executed tests. However, even in the case of significant misalignment, a pre-test calibration procedure could be used to calculate the constant rotation matrix needed to align these two sensors.

Fig. 9. Sensors used to estimate the attitude of FeelHippo AUV.

The Xsens MTi is equipped with a 3-axis accelerometer, a 3-axis gyroscope and a 3-axis magnetometer; in addition, it is equipped with a built-in compass calibration procedure and a proprietary attitude estimation filter. The DSP-1760 FOG, instead, outputs angular rate measurements.

Preliminary tests have been executed to validate the magnetometer calibration procedure introduced in Section III and to evaluate the performance of the proposed filter before using it in extensive navigation trials.

Concerning compass calibration, Figures 10-13 report the results of two suitable calibration tests. The first test was executed in a disturbance-free environment, while before performing the second test a metal object has been placed close to the sensor case. For both tests, the magnetic field

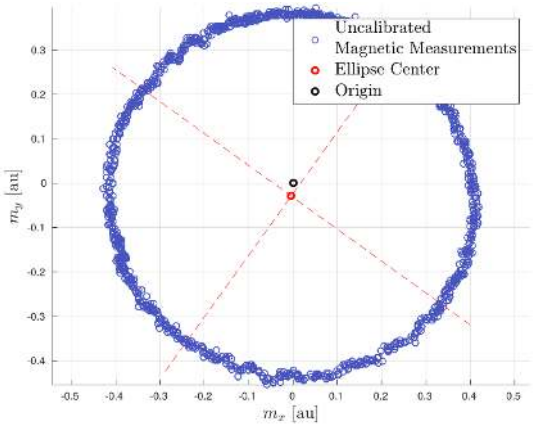

Fig. 10. Undisturbed calibration test: uncalibrated magnetic field.

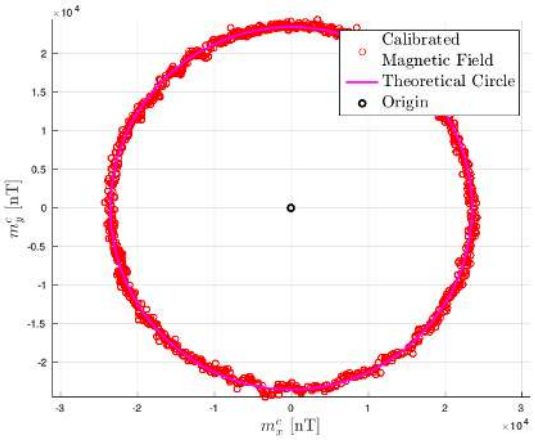

Fig. 11. Undisturbed calibration test: calibrated magnetic field.

measurements collected during a turn of the vehicle about its z-axis are reported, along with the same measurements after the calibration phase (it is worth noting that, in the absence of magnetic disturbances, the readings would lie on a circle centered at the origin of the xy-plane). Figures 10 refers to the first test: the uncalibrated data show that only a minor Hard Iron effect is present, caused by electronics

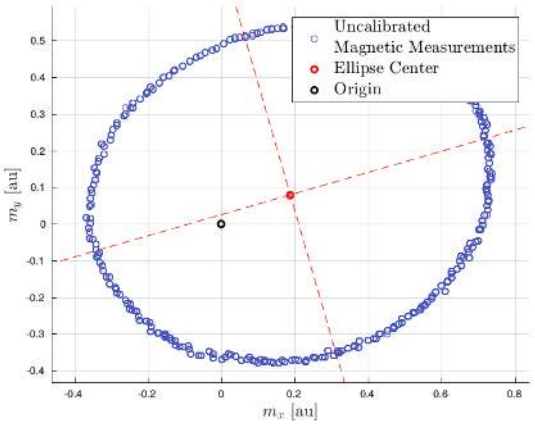

Fig. 12. Disturbed calibration test: uncalibrated magnetic field.

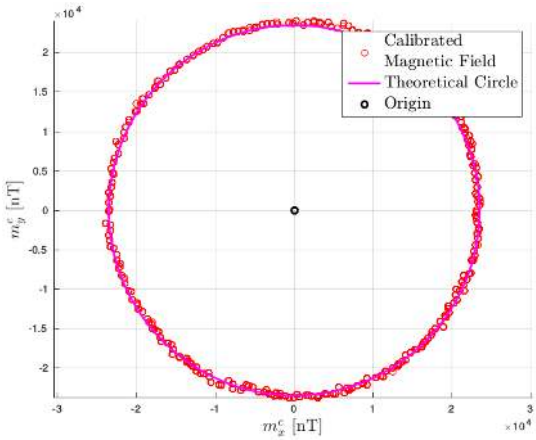

Fig. 13. Disturbed calibration test: calibrated magnetic field.

surrounding the compass housing (which in turn induces a slight shift of the centroid of the measurement locus from the origin). For what concerns the second test (Figure 12), instead, the deviation from the theoretical locus is relevant (indicating the presence of both Hard and Soft Iron disturbances). Nonetheless, Figures 11 and 13 show that, in both situations, the proposed calibration procedure was able to correctly compensate magnetic disturbances, mapping the measurements onto the theoretical locus.

After validating the calibration procedure, suitable tests have been executed to compare the estimate of the proposed filter with the orientation estimated by the Xsens internal filter. The latter is a high-performance estimation filter; in addition, before the development of the proposed solution, it has been extensively and successfully used to perform different sea missions with every AUV of the MDM Lab [19], [20], [21], [22]. Hence, the tests performed aim at verifying that the simple addition of a single-axis FOG (whose price is even inferior to that of a wide range of sensors employed on many underwater vehicles) guarantees a significant performance increase over a commercial state-of-the-art solution. All these tests follow the same procedure: after initializing the filters, a source of magnetic disturbance (i.e. a metal object) is placed close to the IMU while the vehicle is not moving; then, the AUV is rotated about its z-axis together with the disturbance source; finally, the metal object is removed and the vehicle is rotated back to its initial orientation. Figures 14-17 report the results obtained during one of these preliminary tests, assumed as case study. Let

$$\mathbf{\Phi}_d = [\phi_d \ \theta_d \ \psi_d]^T = \mathbf{\Phi}_f - \mathbf{\Phi}_X \tag{26}$$

denote the difference between the roll, pitch and yaw values vector $\mathbf{\Phi}_f$ estimated by the proposed filter and the corresponding quantity $\mathbf{\Phi}_X$ computed by the Xsens algorithm; Figure 14 shows that, while ϕ_d and θ_d remain close to zero, a relevant yaw difference is present. This is due to the Xsens not

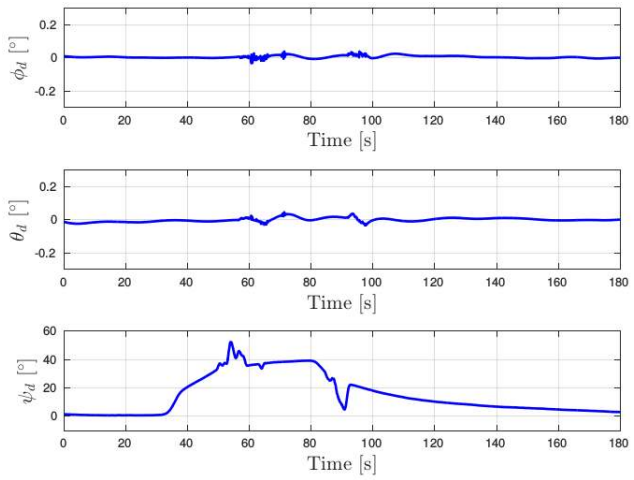

Fig. 14. Components of Φ_{diff} obtained during the preliminary test.

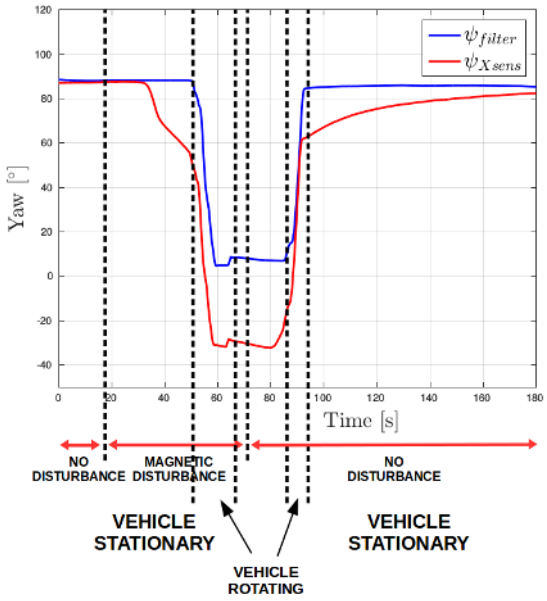

Fig. 15. Yaw values obtained during the preliminary test.

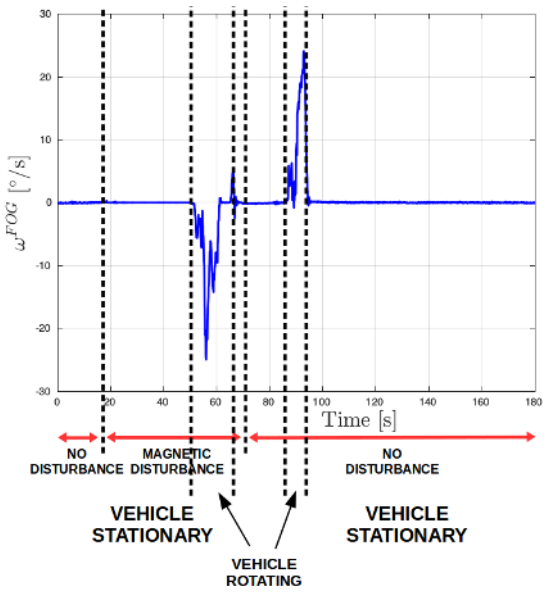

Fig. 16. FOG signal obtained during the preliminary test.

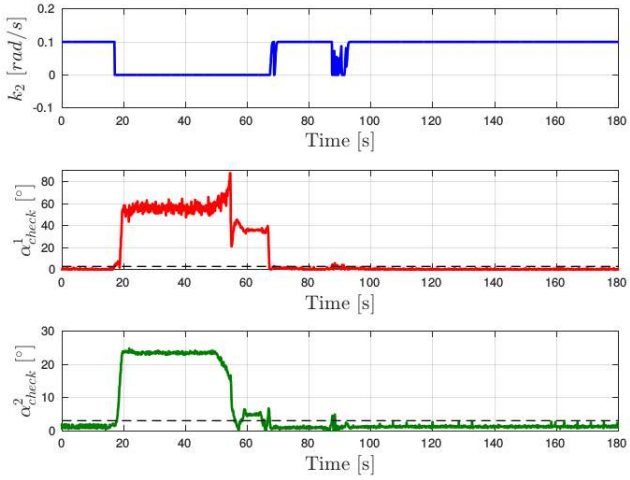

Fig. 17. k_2 and control angle values obtained during the preliminary test.

recognizing the corrupted magnetic measurements, which are employed within its internal filter and result in an incorrect attitude estimate. This is supported by Figure 15 and Figure 16: Figure 15 shows that, after the magnetic disturbance source gets close to the sensor, the yaw estimated by the Xsens filter deviates from the correct value (the FOG signal, reported in Figure 16 to be used as ground truth, indicates that the vehicle has not yet started rotating). On the contrary, the disturbance is correctly identified by the proposed algorithm (the control angles in Figure 17 rapidly exceed the threshold values and the gain k_2 is reduced to zero), and the yaw estimate is computed integrating the FOG rate. Finally, after removing the disturbance source and rotating the vehicle back, the Xsens yaw value slowly converges to the estimate computed by the proposed filter.

After illustrating how the presented estimator is able to cope with unknown magnetic disturbances, its performance has been evaluated during a longer navigation mission. The results reported here refer to one of the tests performed by FeelHippo AUV in the Gulf of Baratti (Livorno, Italy), in shallow water. During the test, the vehicle could experience light marine current; the magnetic characteristics of the location (i.e. the presence of magnetic materials on the sea bottom) were unknown. The vehicle was required to autonomously follow a transept-shaped path, exploiting the attitude estimate computed within its navigation filter. The test was executed on surface; this way, the GPS signal can be used as ground truth.

Figure 18 shows the waypoints of the desired path and the GPS fixes received by the vehicle; Figure 19, instead,

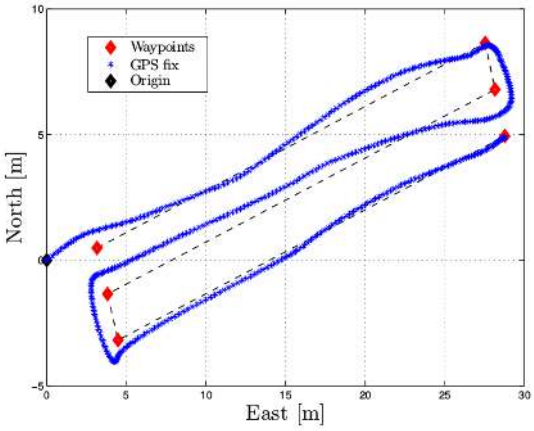

Fig. 18. FeelHippo AUV path.

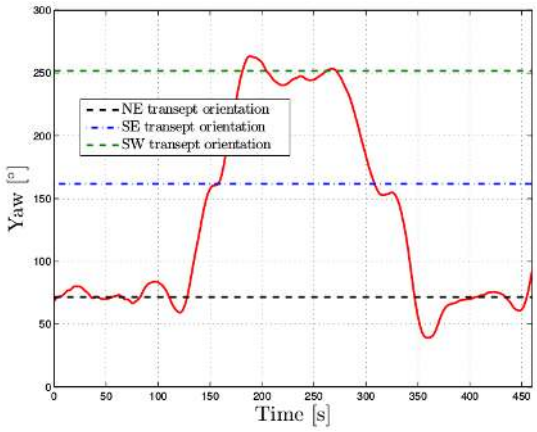

Fig. 19. Yaw estimate.

reports the yaw angle estimated by the filter along with the orientation of the legs of the path (roll and pitch values are very limited due to hydrostatic stability, thus they are not reported). It can be easily seen that the GPS fixes and the estimated yaw show good accordance, indicating that the proposed filter is able to correctly estimate the attitude of the AUV. As regards the compass/FOG usage, Figure 20 shows the values obtained for the magnetometer gain k_2 and for the control angles α^1_{check} and α^2_{check}: in a magnetically-unknown environment, the AUV makes use of both sensors to accurately estimate its attitude. For what concerns the accelerometer measurements, the gain k_1 is fixed at its maximum value for the entire test (since no large accelerations occur), hence it is not shown.
Summarizing, the presented filter is able to compute an accurate estimate of the attitude of an AUV in an a priori unknown environment; the GPS signal, exploited as ground truth, is used to validate the proposed approach and to evaluate its reliability.

VI. Conclusion

This paper focuses on the topic of estimation of the attitude of a mobile robot using a commercial IMU composed of a 3-axis gyroscope, a 3-axis magnetometer and a 3-axis accelerometer. In particular, the underwater field has been considered; nonetheless, the presented solution can be adapted to terrestrial and aerial vehicles as well. Special attention has been given to correctly estimate the yaw angle of the vehicle: such quantity depends indeed on the magnetometer measurements, which are highly susceptible to external disturbance sources.
A suitable attitude estimation filter for an Autonomous Underwater Vehicle (AUV) has been proposed, based on one of the most common attitude estimation algorithms, proposed by Mahony et al. [9] in 2008. The presented filter inherits the structure from Mahony's complementary filter, proposing some design modifications to better suit it to the field of underwater robotics. One of the introduced changes aim at overcoming the problem of the low reliability of the magnetometer measurements, separating correct readings from corrupted ones, discarding the latter and at the same time obtaining an accurate yaw estimate exploiting the readings of an accurate Fiber Optic Gyroscope (FOG). This issue has been addressed with satisfying results.
The performances of the proposed solution have been evaluated; the resulting filter has been used to estimate the attitude of an AUV during the execution of an autonomous navigation task. The obtained results are satisfying; the proposed algorithm is capable of computing an accurate estimate of the vehicle orientation: in particular, a reliable estimate of the yaw angle, which is fundamental to navigation, is available even in a magnetically unknown environment. Thus, the presented solution is able to overcome the limitations imposed by the high susceptibility of commercial IMUs to external magnetic disturbances.

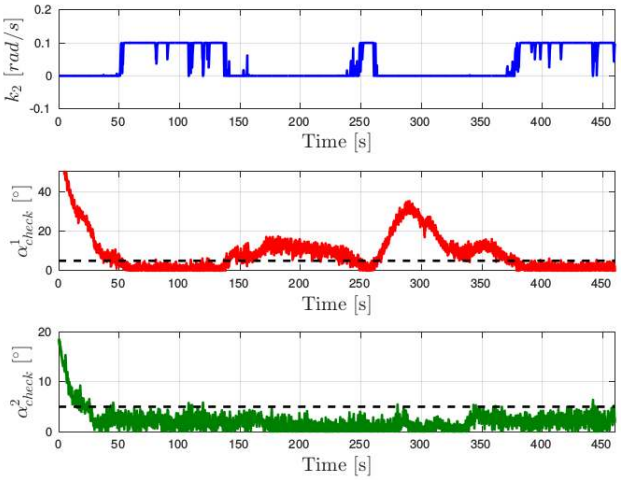

Fig. 20. k_2 and control angles values.

Acknowledgments

This work has been partially supported by the European ARROWS project (this project has received funding from the European Union's Seventh Framework Programme for Research technological development and demonstration, under grant agreement no. 308724) and by the SUONO

project (Safe Underwater Operations iN Oceans), ranked first in the challenge on "Sea Technologies" of the competitive call named "Smart Cities and Communities" issued by the Italian Ministry of Education and Research. The authors would really like to thank Texas Instruments© which provided FeelHippo motors drivers. Finally, the authors would like to thank their colleagues of the MDM Lab of the University of Florence for the support during the research projects and the UNIFI Robotic Team which participated in euRathlon 2015 competition for the help received in setting up the vehicle.

References

[1] Kalman R.E., *A New Approach to Linear Filtering and Prediction Problems*, Trans. of the ASME Journal of Basic Engineering, Vol. 82, Series D, pp 35-45 (1960).

[2] Bar-Shalom Y., Li X.R., Kirubarajan T., *Estimation with Applications to Tracking and Navigation: Theory Algorithms and Software*, Wiley, Jul. (2001).

[3] Julier S.J., Uhlmann J.K., *A New extension of the Kalman Filter to Nonlinear Systems*, in Proceedings of the SPIE Signal Processing, Sensor Fusion and Target Recognition VI Conference, Vol. 3068, Jul. 28 (1997).

[4] P. Batista, C. Silvestre, P. Oliveira, *Sensor-Based Globally Asymptotic Stable Filters for Attitude Estimation: Analysis, Design, and Performance Evaluation*, IEEE Trans. on Automatic Control, Vol. 57, N. 8, Aug. (2012).

[5] N. Trawny, S.I. Roumeliotis, *Indirect Kalman Filter for Attitude Estimation*, Dept. of Computer Science & Engineering, Technical Report, Vol. 2, Mar. (2005).

[6] Aghili F., Salerno A., *Driftless 3-D Attitude Determination and Positioning of Mobile Robots By Integration of IMU With Two RTK GPSs*, IEEE/ASME Transactions on Mechatronics, Vol. 18, Issue 1, pp. 21-31, Aug. (2011).

[7] J.L. Crassidis, *Sigma-Point Kalman Filtering for Integrated GPS and Inertial Navigation*, AAIA Guidance, Navigation and Control Conference and Exhibit, San Francisco (CA), Aug. 15-18 (2005).

[8] Euston M., Coote P., Mahony R., Kim J., Hamel T., *A Complementary Filter for Attitude Estimation of a Fixed-Wing UAV*, IEEE/RSJ International Conference on Intelligent Robots and Systems, Nice (FR), Sept. 22-26 (2008).

[9] Mahony R.E., Hamel T., Pflimlin J.M., *Nonlinear Complementary Filters on the Special Orthogonal Group*, IEEE Trans. on Automatic Control, Vol. 53, N. 5, pp 1203-1218 (2008).

[10] Allotta B., Costanzi R., Fanelli F., Monni N., Ridolfi A., *Single axis FOG aided attitude estimation algorithm for mobile robots*, Mechatronics, Vol. 30, pp. 158-173 (2015).

[11] Fossen T.I., *Guidance and Control of Ocean Vehicles*, 1st ed., John Wiley & Sons, Chichester UK (1994).

[12] Siciliano B., Khatib O., *Handbook of Robotics*, Springer Handbooks, Napoli and Stanford (2008).

[13] Vasconcelos J.F., Elkaim G., Silvestre C., Oliveira P., Cardeira B., *A Geometric Approach to Strapdown Magnetometer Calibration in Sensor Frame*, IEEE Transactions on Aerospace and Electronics Systems, Vol. 47, N. 2, pp. 1293-1306, Apr. (2011).

[14] Kok M., Schön T.B., *Maximum likelihood calibration of a magnetometer using inertial sensors*, in Proceedings of the 19th World Congress of the International Federation of Automatic Control (IFAC), pp. 92-97, Cape Town (SA), Aug. (2014).

[15] Gebre-Egziabher D., Elkaim G., David Powell J., Parkinson B., *Calibration of Strapdown Magnetometers in Magnetic Field Domain*, Journal of Aerospace Engineering, Vol. 19, Issue 2, Apr. (2006).

[16] National Geophysics Data Center, *http://www.ngdc.noaa.gov*

[17] Hua M.-D., Rudin K., Ducard G., Hamel T., Mahony R., *Nonlinear attitude estimation with measurement decoupling and anti-windup gyro-bias compensation*, in Proceedings of the 18th IFAC World Congress 2011 (IFAC 2011), pp. 2972-2978, Milano (IT), Aug. 28 - Sept. 2 (2011).

[18] Martin P., Salaün E., *Design and implementation of a low-cost observer-based attitude and heading reference system*, Elsevier Control Engineering Practice, Vol. 18, Issue 7, pp. 712-722, July (2010).

[19] Allotta B., Costanzi R., Meli E., Pugi L., Ridolfi A., Vettori G., *Cooperative localization of a team of AUVs by a tetrahedral configuration*, Robotics and Autonomous Systems, Vol. 6, N. 8, pp. 1228-1237, Aug. (2014).

[20] Allotta B., Bartolini F., Costanzi R., Monni N., Pugi L., Ridolfi A., *Preliminary design and fast prototyping of an autonomous underwater vehicle propulsion system*, in Proceedings of the Institution of Mechanical Engineers, Part M: Journal of Engineering for the Maritime Environment, Vol. 229, N. 3, pp. 248-272, Aug. (2015).

[21] Allotta B., Caiti A., Costanzi R., Fanelli F., Fenucci D., Meli E., Ridolfi A., *A new AUV navigation system exploiting unscented Kalman filter*, Ocean Engineering, Vol. 113, pp. 121-132 (2016).

[22] Allotta B. et al., *The ARROWS project: adapting and developing robotics technologies for underwater archaeology*, in Proceedings of the IFAC Workshop on Navigation, Guidance and Control of Underwater Vehicles (NGCUV 2015), Girona, Spain, Apr. (2015).